Coupled Brillouin-Raman study of direct and folded acoustic modes in GaAs-AlAs superlattices

J. Sapriel and J. He

Laboratoire de Bagneux, Centre National d'Etudes des Télécommunications, 196 avenue Henri Ravera, 92220 Bagneux, France

B. Djafari-Rouhani

Laboratoire de Physique du Solide, Faculté des Sciences et Techniques, Université de Haute Alsace, 2 rue des Frères Lumière, 68093 Mulhouse Cédex, France

R. Azoulay

Laboratoire de Bagneux, Centre National d'Etudes des Télécommunications, 196 avenue Henri Ravera, 92220 Bagneux, France

F. Mollot

Laboratoire de Microélectronique et Microstructures, Centre National de la Recherche Scientifique, 196 avenue Henri Ravera, 92220 Bagneux, France

(Received 6 July 1987)

Acoustic and acousto-optic properties are investigated in GaAs-AlAs superlattices of period D ranging between 40 and 500 Å. An experimental setup where a Fabry-Perot interferometer is used in tandem with the Raman spectrometer allowed frequency-shift measurements as low as 1 cm^{-1}. The dispersion branches of (direct) LA and TA, as well as folded-LA and -TA, modes are obtained for excitation wave vectors q less than the limit π/D of the first Brillouin zone, and in the range π/D to $2\pi/D$ (second Brillouin zone). The intensities of all these modes are very sensitive to the reduced excitation wave vector $Q = qD/\pi$. Many striking effects are pointed out for the first time: The existence of folded acoustic branches which are observed at frequencies below the direct acoustic branch for $Q > 1$, and the "anomalous" intensity behavior, certain modes becoming even more intense than the Brillouin line for Q approaching the Brillouin-zone limit $Q = 1$. Determination of the relative value p of the Pockels photoelastic coefficient p_{13} in AlAs with respect to GaAs is also reported. p is observed to undergo a noticeable variation versus the photon energy between 6764 and 4579 Å.

I. INTRODUCTION

This is the report of a systematical investigation of the acoustic phonons in GaAs-AlAs superlattices. The phonons under study are either direct acoustic phonons, as those which could be observed in a Brillouin scattering experiment, or folded acoustic phonons, as usually probed by the Raman techniques and which are due to the superperiod D in the direction of growth z. Most of the experiments presented here are compared to the results of a recent theoretical study[1] on the intensity of this kind of phonon mode in a very large range of scattering-wave-vector values. In this theory the modulation of the acoustic, optic, and photoelastic properties in the superlattice are taken into account and for the first time both the interacting optic and acoustic waves are treated as Bloch functions. One will also find in Ref. 1 a thorough comparison between this improved model of scattering from acoustic modes and previous ones, in the case of GaAs-AlAs superlattices.

Several Raman studies in (001)-oriented GaAs-AlAs superlattices have been devoted to the investigation of the folded-longitudinal-acoustic modes (FLA).[2–4] However, all of them have been limited to phonon excitation wave

vectors less than the Brillouin-zone edge π/D, thus missing some interesting frequency and intensity behaviors which are related in this paper.

In our study we have mainly focused on long-period GaAs-AlAs superlattices and in many cases the phonon excitation wave vectors exceed the Brillouin-zone edge. Using a new experimental setup combining the advantages of both Raman and Brillouin techniques, we have been able to investigate the direct LA and TA modes, as well as the FLA and FTA (folded-transverse-acoustic modes). A study of the FTA in GaAs-AlAs superlattices has been reported recently,[5] but nothing has been published on the LA and TA modes, as the only Brillouin study of the literature has focused on the Rayleigh surface acoustic waves (RSW) propagating parallel to the layers.[3]

The case where the phonon excitation wave vector q is larger than π/D, also called the umklapp process, has been investigated in Si/Ge$_x$Si$_{1-x}$ superlattices by Dharma-wardana *et al.*[6] In this system, the frequencies of the modes are higher than those of the corresponding modes in GaAs-AlAs superlattices, due to larger values of the acoustic velocities in the constitutive layers (for instance, the Brillouin line is $\simeq 5$ cm^{-1} in Si/Ge$_x$Si$_{1-x}$

though its shift is only $\simeq 2.5$ cm^{-1} in GaAs/AlAs). Thus the low-frequency modes are more difficult to observe in GaAs-AlAs superlattices. Actually our experimental set-up, where a Fabry-Perot interferometer is used in conjunction with a Raman spectrometer, allows the determination of modes corresponding to frequency shifts as low as 1 cm^{-1}. We could thus observe folded acoustic modes of frequency even lower than the Brillouin mode, whose existence have been predicted in Ref. 1 for phonon excitation wave vector q larger than π/D. (Actually this feature had not been explicitly pointed out before, though it could be deduced from the equations contained in Ref. 6.)

The FLA, which are allowed modes in our scattering geometry, are particularly investigated and their intensities are measured with respect to the corresponding Brillouin LA (considered as a reference). Such measurements have been performed for several samples in different experimental situations characterized by different values of the scattering wave vector. The experimental results are compared to the theoretical predictions (Sec. III). In the theoretical study we assumed a perfect periodicity and square-wave-like modifications of the physical properties from one layer to the other. The deviation from strict periodicity as well as the optical-absorption effects are briefly discussed in Sec. IV, as well as their incidence on the linewidths. But before coming to the heart of the matter let us first give a brief description of the "folding" effect of acoustic phonons in superlattices (Sec. II).

II. BASES OF THE FOLDING EFFECT

In this section we recall some general features of the folded acoustic modes in the elastic approximation and we generalize them to experimental situations where the scattering wave vector is larger than the Brillouin-zone dimension π/D.

The frequencies of the phonons involved in the scattering process depend on the phonon excitation wave vector q which is given by $q = k_s - k_i$; here k_s and k_i are the wave vectors of the incident and scattered light, respectively. For backscattering $k_s \simeq -k_i$ and $q = 2 \mid k_i \mid = 4\pi N/\lambda$, N being the refractive index of the superlattice for the laser radiation of wavelength λ in the vacuum. The phonons involved in the scattering process correspond to a wave vector k given by

$$k = q + 2\pi m/D \ . \tag{1}$$

Here m is a positive or negative integer.

The circular frequencies ω of the folded acoustic modes as a function of k are given by the implicit equation:[7]

$$\cos(kD) = \cos\left[\frac{\omega d}{v}\right] \cos\left[\frac{\omega d'}{v'}\right]$$
$$- \frac{1}{2}\left[\frac{\rho v}{\rho' v'} + \frac{\rho' v'}{\rho v}\right] \sin\left[\frac{\omega d}{v}\right] \sin\left[\frac{\omega d'}{v'}\right] \ . \tag{2}$$

Here d and d' are the thickness of the layers whose densities are ρ and ρ' and whose acoustic velocities are v and

v'. The dispersion curves of Eq. (1) can actually be approximated by taking $\rho v = \rho' v'$. In these conditions one obtains from (2)

$$\omega = V \left| q + \frac{2\pi}{D} m \right| \ , \tag{3}$$

V being a mean velocity $(D/V = d/v + d'/v')$. $m = 0$ corresponds to the direct acoustic mode (Brillouin line); $m = \pm 1, \pm 2, \pm 3, \ldots$, are associated to the folded acoustic branches which we label (FLA)$_m$ or (FTA)$_m$, according to their folding index m, and their acoustic polarization (LA or TA). Changing q in $q + 2\pi p/D$ (p integer) one obtains the same value for ω, but now the corresponding phonon branches have to be labeled differently; their folding index transforms from m to $m - p$ (see Fig. 2 of Ref. 1).

It is sometimes more convenient to express Eq. (3) in a standard form, which is valid irrespective of the period D and contains only dimensionless parameters.

If one writes $\Omega = \omega D/2\pi c$ and $Q = qD/\pi$, one obtains from Eq. (3)

$$\Omega = \frac{V}{c} \mid Q/2 + m \mid \ . \tag{3'}$$

Q is the reduced phonon excitation wave vector; c is the light velocity in vacuum, and $\Omega = \Delta v\, D$; Δv being the phonon mode energy expressed in cm^{-1} (D is then expressed in cm).

For $Q > 1$, i.e., $\lambda < 2ND$, the direct acoustic branch ($m = 0$) is not the lowest-frequency branch (as for $Q < 1$). Certain folded acoustic branches lie below the acoustic branch. For instance, for $1 < Q < 2$, the (FLA)$_{-1}$ displays a lower frequency than the LA; for $2 < Q < 3$, (FLA)$_{-1}$ is still below the LA, and the (FLA)$_{-2}$ branch is between the (FLA)$_{-1}$ and LA branches (see Fig. 2 of Ref. 1).

It is worthwhile noting that Q values are not limited to 1 as considered before, but the parameter Q is defined in an extended Brillouin zone which is theoretically unlimited, since the intensity of the different modes is not a periodic function of Q (contrary to the phonon frequencies). Yet, experimentally the range of Q is limited to 3 or 4 since one increases Q chiefly by increasing D, thus creating a high density of overlapping folded modes.

Roughly speaking, the intensities of FLA modes have a general tendency to decrease with the $\mid m \mid$ values and the Brillouin line ($m = 0$) is the most intense mode. But actually the intensity behavior varies drastically with Q. According to Ref. 1, certain FLA modes can be much more intense than the Brillouin line for Q close to integer values.

III. EXPERIMENTAL RESULTS

As the superlattice crystals are absorbing materials for the radiations of the lasers (krypton and argon ion), the light is collected in the backscattering geometry. The stray light corresponding to elastic scattering is then relatively important even for a double- or triple-grating Raman spectrometer, thus limiting the signal observed in good experimental conditions to frequencies above 5

cm^{-1}. A clear improvement of the resolution and contrast has been obtained by interposition of a plane Fabry-Perot interferometer (PFP) between the sample and our Ramanor U 1000 double monochromator from Jobin-Yvon. The distance between the two plates of the PFP is 1 mm; the PFP is scanned by variable pressure flow of CO_2 gas and approximately two spectral ranges are probed. The finesse $F \simeq 40$ leads to a contrast of about 10^3 for the PFP. Two methods are available to perform the measurements. The first one consists of using the Raman spectrometer as a filter whose maximum transmission is fixed at the frequency of the line under investigation though only the PFP is scanned. The bandwidth of the monochromator which depends on the slit's aperture is taken large with respect to the width of the line in order to avoid deformation of its profile. The whole system (Raman spectrometer and PFP) (see Fig. 1) displays a high resolution ($\simeq 0.15$ cm^{-1}) with a good optical transmission since the slit widths of the Raman spectrometer are kept relatively large ($\simeq 100$ μm). The frequency is precisely measured by recording a reduced Rayleigh line as reference in the spectra.

Another technique consists of synchronizing the scans of both the Raman spectrometer and the PFP in order to record several lines in the available range of 10 cm^{-1} obtained during a cycle of variations of the gas pressure, thus allowing direct measurement of the relative intensities of the different modes.

This study has been carried out on about 12 GaAs-AlAs superlattice samples of different compositions and periods. We selected here the results on the most representative of them, whose characteristics are reported in Table I. The frequency and the peak intensity of the direct and folded acoustic modes are investigated here, as a function of the excitation wave vector. The linewidth will be considered later on, and the modification brought to the intensity by the different causes of phonon mode broadening will be analyzed accordingly (see Sec. IV).

One can distinguish TA modes from LA modes in the

TABLE I. Characteristics of the investigated superlattices made of alternating layers of GaAs and AlAs of thicknesses d and d', respectively. $D = d + d'$ is the superlattice period. All these samples have large D values, except sample V. Samples II–V have approximately the same aluminum concentration x and differ in their period (the acoustic mode frequencies are given in Fig. 6).

Sample	D (Å)	$x = d'/D$
I	376	0.45
II	187	0.74
III	421	0.73
IV	474	0.78
V	40.5	0.74

experiments since they correspond to different selection rules of the light polarizations. LA and FLA modes can be seen only if the polarizations of the incident and scattered light are parallel (A_1 symmetry). In the other geometry (crossed polarizations) only the TA and FTA appear. In Fig. 2 are shown the first FTA modes obtained with crossed polarizations in sample II.

Let us now give a short description of a few typical low-frequency spectra obtained on our superlattice samples, which summarizes the main features of the frequency and intensity behavior of the different modes. Spectra corresponding to sample I (gallium-rich) and to sample III (aluminum-rich superlattices) are given in Figs. 3 and 4, respectively, for different values of the reduced excitation wave vector Q. In Fig. 3(a) ($Q = 0.78$) one can notice that the LA and $(FLA)_{-1}$ modes have approximately the same intensity, though the $(FLA)_{+1}$ mode is much less intense. This intensity behavior [strong asymmetry on the components -1 and $+1$ of the first folded-longitudinal-acoustic doublet, drastic increase of the $(FLA)_{-1}$ with respect to the Brillouin line] has been pre-

FIG. 1. Schematic arrangement of the experimental setup. A single-pass plane Fabry-Perot (PFP) and a double-grating Raman spectrometer are used in tandem. The sample S is kept in vacuum to avoid the superposition of Raman lines from air. The PFP is scanned by CO_2 gas pressure variations. A photomultiplier with a photon counter is used for detection.
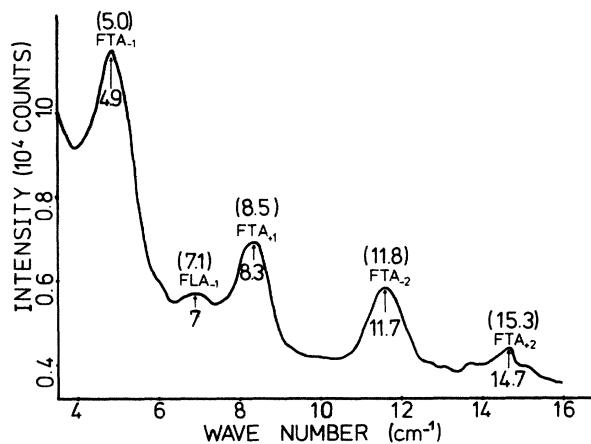
FIG. 2. Scattering from folded-transverse-acoustic modes (FTA) for crossed polarizations of the incident and scattered light in sample II. The FLA for $\lambda = 5145$ Å modes are not allowed in this geometry, but a residual line is, however, observed. The measured frequencies are reported below the peaks. The calculated ones obtained from Eq. (2) are indicated in parentheses.
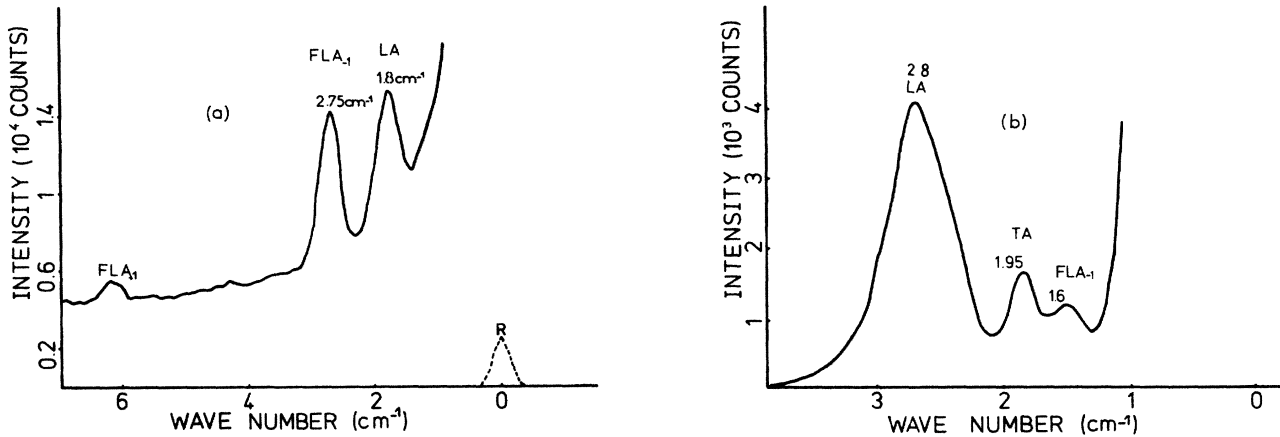
FIG. 3. Light scattering in sample I for different Q values obtained by changing the light wavelength λ. (a) For $\lambda = 6764$ Å (krypton laser), $Q = 0.78$, one observes a $(FLA)_{-1}$ peak more intense than the Brillouin line. Besides, one can notice that $(FLA)_{+1}$ is much less intense than $(FLA)_{-1}$. (b) For $\lambda = 4765$ Å (argon-ion laser), $Q = 1.28$. The scattering wave vector is in the second Brillouin zone. A new mode is seen below the LA, whose assignment is $(FLA)_{-1}$. The TA mode is also noticed, due to a polarization leakage caused by the Brewster incidence.
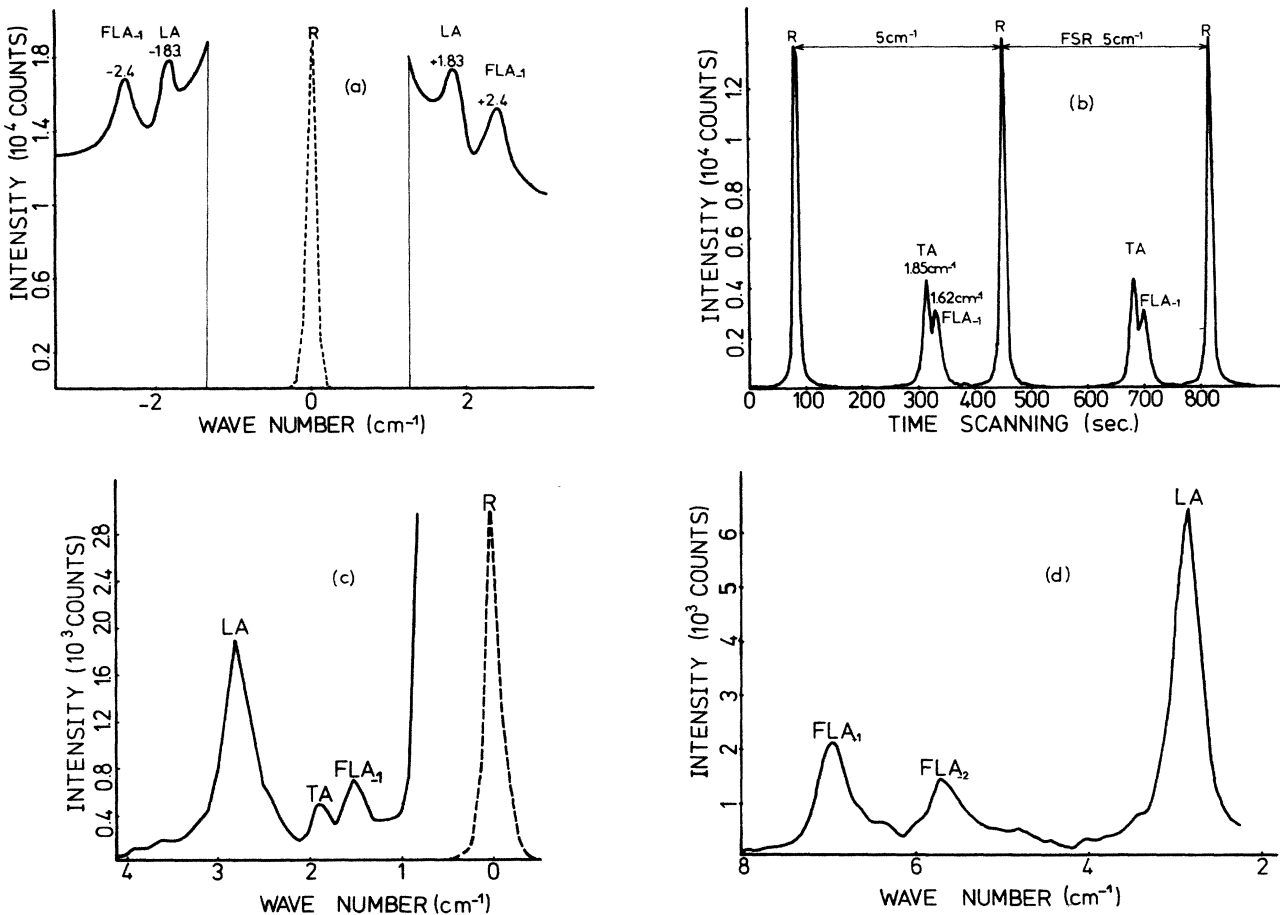
FIG. 4. Spectra corresponding to an aluminum-rich superlattice (sample III). (a) For $\lambda = 6471$ Å, $Q = 0.86$ one observes, in spite of an intense background, probably due to luminescence, the $(FLA)_{-1}$ and LA with comparable intensities in Stokes and anti-Stokes scattering. (b) For $\lambda = 4880$ Å, $Q = 1.26$. Here the Raman spectrometer acts as a filter whose maximum transmission is shifted with respect to the laser line by 1.75 cm^{-1}. The Fabry-Perot is scanned and one can observe the TA and $(FLA)_{-1}$ which are very close, but are nevertheless separated owing to the good resolution of the experimental setup. Two free spectral ranges are observed. One can notice the periodicity of the figure, which is a good check of the linearity of the scan. (c) and (d) for $\lambda = 4765$ Å, $Q = 1.36$, at frequencies from both sides of the Brillouin LA.

dicted.[1] For Q values tending to 1 in the first Brillouin zone the intensity of the $(FLA)_{-1}$ increases markedly with respect to the Brillouin line, and for Q values close to 1, one can only observe the $(FLA)_{-1}$. This is also quite consistent with the energy theory of Ref. 1. The modes below the LA are shown in Fig. 3(b) for $Q = 1.28$; one can clearly observe the TA and a small peak at 1.6 cm^{-1} corresponding to $(FLA)_{-1}$. Similar observations on sample III are reported for $Q = 0.86$ [Fig. 4(a)], $Q = 1.26$ [Fig. 4(b)] and $Q = 1.32$ [Figs. 4(c) and 4(d)]. In Fig. 4(a) the LA and $(FLA)_{-1}$ whose intensities are quite comparable are superposed to an intense background. In the experimental conditions of Fig. 4(b), the Raman spectrometer is fixed at 1.75 cm^{-1} and acts as a filter, though the PFP is scanned. Two free spectral ranges are thus described. Two peaks separated by 0.23 cm^{-1} are resolved by the experimental setup and assigned to the TA and the $(FLA)_{-1}$. Both modes correspond to frequency shift smaller than the Brillouin line. For $Q = 1.32$, a few modes are also shown above [Fig. 4(d)] and below the Brillouin LA [Fig. 4(c)].

All the frequency measurements concerning samples II–V, which correspond to different periods, but to approximately the same composition ($x = 0.74$) are brought together, and the synthesis of all the results is presented in the form of standard dispersion curves of the lowest LA and TA branches in the acoustic range (see Fig. 5). Ω and Q are dimensionless parameters defined here above, and they are theoretically related by Eqs. (1) and (2). The experimental points are obtained for reduced excitation wave vectors in the first Brillouin zone ($Q < 1$) and second Brillouin zone ($1 < Q < 2$). The dispersion
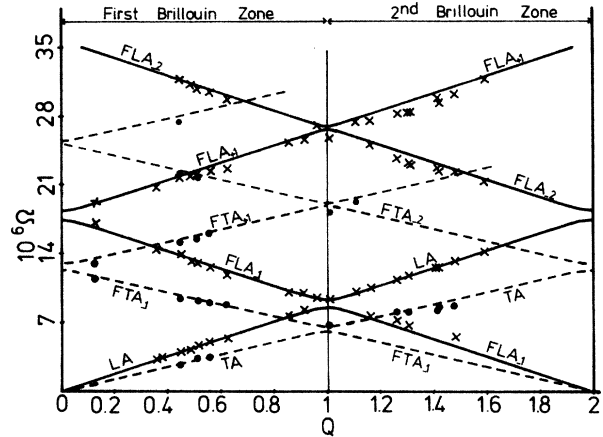
FIG. 5. Normalized frequency Ω of the LA, TA, FLA, and FTA modes as a function of the reduced scattering wave vector Q for samples II–V, which correspond to nearly the same aluminum concentration. One can notice the existence of a folded-longitudinal-acoustic branch at frequency lower than the Brillouin LA. The variations of Q are obtained by changing the laser line wavelengths λ in the range 4500–7000 Å. One has $Q = 4ND/\lambda$ for the experimental conditions (backscattering). Here N is an effective refractive index; one has $DN^2 = dn^2 + d'n'^2$ where d,d' and n,n' are the thicknesses and refractive indexes of the constitutive layers (Ref. 11). One can notice that the experimental points ($\times$ for longitudinal modes and ● for transverse modes) are very close to the calculated curves obtained from the elastic model (solid line for longitudinal branches and dashed line for transverse ones). The data on GaAs and AlAs refractive indexes taken from Ref. 12 as well as the elastic constants of GaAs. The elastic constants of AlAs are assumed equal to those of GaAs.

TABLE II. Comparisons between the experimental results and theory (Ref. 1). We have taken $P = n'^4 p'_{13}/n^4 p_{13}$ with n',n, and p',p the refractive index and the photoelastic constants in AlAs and GaAs, respectively. The measurements have been performed at $\lambda = 4880$ Å for different values of $Q > 1$; it can be seen that $P = 0.15$ corresponds to the best fit between theory and experiments.

Samples	Modes	Calculated frequency (cm^{-1})	Measured frequency (cm^{-1})	Calculated intensity $P = 0.1$	$P = 0.15$	$P = 0.2$	Measured intensity
IV	$(FLA)_{-1}$	1.13	1.20	0.386	0.289	0.221	0.30
($Q = 1.41$)	LA	2.67	2.68	1	1	1	1
	$(FLA)_{-2}$	4.94	4.71	0.268	0.201	0.153	0.23
	$(FLA)_{+1}$	6.48	6.2	0.423	0.303	0.220	0.30
	$(FLA)_{-3}$	8.73	8.3	0.092	0.067	0.050	0.04
	$(FLA)_{+2}$	10.28	9.9	0.171	0.123	0.089	0.12
III	$(FLA)_{-1}$	1.54	1.58	0.316	0.239	0.181	0.22
($Q = 1.27$)	LA	2.69	2.68	1	1	1	1
	$(FLA)_{-2}$	5.79	5.60	0.185	0.143	0.112	0.17
	$(FLA)_{+1}$	6.93	6.7	0.381	0.284	0.213	0.30
	$(FLA)_{-3}$	10.01	9.8	0.020	0.015	0.011	0.02
	$(FLA)_{+2}$	11.18	10.8	0.097	0.072	0.054	0.09
I	$(FLA)_{-1}$	1.74	1.68	0.150	0.125	0.103	0.13
($Q = 1.23$)	LA	2.77	2.73	1	1	1	1
	$(FLA)_{-2}$	6.27		0.002	0.002	0.002	not seen
	$(FLA)_{+1}$	7.28	7.2	0.148	0.124	0.102	0.13
	$(FLA)_{-3}$	10.79	10.4	0.012	0.010	0.009	0.01

branches drawn in solid lines (LA and FLA modes) and dashed lines (TA and FTA modes) are calculated from Eq. (2). The experimental points are reported as a function of Q. Most of them correspond to longitudinal modes (crosses) but one can also distinguish transverse modes (solid circles) which are in principle forbidden but are nevertheless observed because of a polarization leakage[5] due to Brewster incidence. The 457.9-, 465.8-, 472.7-, 476.5-, 488-, 501.7-, and 514.5-nm excitation wavelengths of the argon-ion laser were used, as well as the 530.9-, 568.2-, 647.1-, and 676.4-nm krypton laser lines. One can notice in Fig. 5 the good agreement between experiments and theory for all the investigated branches.

It is now worthwhile to make a quantitative comparison between theory and experiments and more especially, deducing the relative photoelastic constants of GaAs and AlAs involved in the scattering process. If one labels z (or 3) the superlattice growth direction, these photoelastic constants are the Pockels coefficients p_{13} and p'_{13} according to Nye notations.[8] It is sometimes easier to carry out the notations P_{13} used in Ref. 2 where $P_{13} = -n^4 p_{13}$ and $P'_{13} = -n'^4 p'_{13}$, where n and n' are the refractive index and p_{13}, p'_{13} the Pockels constants of GaAs and AlAs, respectively. In Ref. 1 it has been pointed out that the relative intensity of the different folded modes with respect to the intensity of the Brillouin line is quite sensitive to the ratio $P = P'_{13}/P_{13}$. In Table II we have reported both the results of the experiments and the results of the calculations. The intensities of the modes are taken with the Brillouin line as a reference for three superlattice samples. The numerical results for the intensities are performed by taking several values of P ($P = 0.1$, $P = 0.15$, $P = 0.2$). Comparisons between the experiments performed at $\lambda = 4880$ Å (blue line of the argon laser) and the calculated values allow a correct determination of P; thus one obtains $P = 0.15 \pm 0.015$ for $\lambda = 4880$ Å. In Table III we have reported the calculated intensities for different values of p and λ, as well as the peak intensities for sample II. Comparisons between the eighth column and the fifth, sixth, and seventh columns confirm the value of $P = 0.15$ for $\lambda = 4880$ Å. Besides, one finds $P = 0.1 \pm 0.015$ for $\lambda = 6764$ Å (krypton laser

line) and $P = 0.2 \pm 0.015$ for $\lambda = 4579$ Å (argon-ion laser). Obviously, there is a dispersion effect of the P versus λ; this effect is still more clear when one considers the ratio of the Pockels constant p_{13}; one finds $p'_{13}/p_{13} = 0.23$ for $\lambda = 6764$ Å, 0.43 for $\lambda = 4880$ Å, and 0.66 for $\lambda = 4579$ Å.

IV. DISCUSSION

In this paper, the ratios of the intensities of the different modes have been measured peak to peak and the experimental values have been compared to the theory. Actually, the theory of light scattering by acoustic phonons has been established for perfectly homogeneous superlattices with abrupt interfaces; the optical-absorption effects have not been considered. Let us examine now the consequence of the different line broadening causes on the intensities. Variations of the superlattice period inside the probed zone are an example of inhomogeneities which can occur. The effect of these variations (of the order of a few monolayers) is to broaden the peaks and to reduce their peak height accordingly. Clearly this broadening is frequency dependent and thus increases with the folding index. In addition, long-period superlattices are less affected by these variations than short-period superlattices. Therefore one can expect better agreement between theory and peak-to-peak intensity measurements for low-frequency modes in long-period superlattices, as those probed in this paper. For folded acoustic modes corresponding to higher frequencies which are more sensitive to the defects, one has to consider the integrated intensities of the peaks. As to the optical absorption, the induced broadening is approximately given[9] by $2\alpha_{op}V$ (α_{op} is the optical absorption, V is the acoustic velocity in the superlattice) and all modes are affected in the same way and have nearly the same width. Thus the relative intensity of the modes is not modified and it is not necessary to consider the optical absorption when one deals with relative measurements.

Let us now discuss the value of p'_{13}/p_{13}, determined by fitting our experimental results on several folded acoustic modes with the theory. It is likely that the photoelastic constants of GaAs (AlAs) layers take the same value in the superlattice structure as in bulk GaAs (AlAs) for

TABLE III. Same as Table II, but for sample II and for different laser lines.

$\lambda_{(nm)}$	Modes	Calculated frequency (cm^{-1})	Measured frequency (cm^{-1})	Calculated intensity			Measured intensity
				$P = 0.1$	$P = 0.15$	$P = 0.2$	
457.9 ($Q = 0.63$)	LA	2.99	2.9	1	1	1	1
	(FLA)$_{-1}$	6.58	6.3	0.479	0.357	0.270	0.27
	(FLA)$_{+1}$	12.59	12.1	0.447	0.320	0.232	0.22
488.0 ($Q = 0.56$)	LA	2.67	2.7	1	1	1	1
	(FLA)$_{-1}$	6.89	6.8	0.451	0.334	0.252	0.31
	(FLA)$_{+1}$	12.27	12.0	0.449	0.321	0.233	0.29
676.4 ($Q = 0.36$)	LA	1.72	1.75	1	1	1	1
	(FLA)$_{-1}$	7.84	7.7	0.389	0.285	0.212	0.40
	(FLA)$_{+1}$	11.33	11.1	0.470	0.338	0.246	0.45

laser excitation radiations far from the electronic transitions. Actually the measurements performed in several superlattice samples (see Tables II and III) confirm that the ratio p'_{13}/p_{13} is not sample dependent for $\lambda = 4880$ Å. The situation seems to be different for laser radiations of energy $\simeq 1.85$ eV (red lines of the krypton laser). To these light wavelengths correspond electronic levels of GaAs quantum wells. In resonance conditions, it is likely that the photoelastic constants undergo a substantial increase in the GaAs slabs. A similar enhancement has been observed and analyzed on the optical mode intensities.[10] It is therefore not surprising to find a value of the ratio p'_{13}/p_{13} in sample II ($d = 45$ Å) smaller for $\lambda = 6764$ Å since the resonance effect occurs for p_{13} though p'_{13} of AlAs is not affected, the electrons being confined in the GaAs layers. Thus one can distinguish between values of p'_{13}/p_{13} at light energies far from electronic transitions which are sample independent in GaAs-AlAs superlattices, and p'_{13}/p_{13} values at energies close to electronic transitions which depend on the thickness of the GaAs slabs, acting as multiple quantum wells.

V. CONCLUSION

In spite of the drawback due to the very low frequency of the acoustic modes in GaAs-AlAs superlattices, we have performed a systematic and thorough investigation of these modes, owing to the good sensitivity and the high contrast and resolution of our experimental setup. Several striking features of their frequencies and intensi-

ties in the backscattering geometry are pointed out, especially for periods larger than the critical value $D_0 = \lambda/4N$. Though the transverse modes are not allowed in the scattering geometry used here, we have shown that there is no insuperable hindrance to their study. According to Ref. 1 the region close to $Q = 2$ is characterized by a particularly "abnormal" behavior of the relative intensities of the modes, due to the proximity of the light Bragg reflection. Indeed it is worthwhile investigating this region, but due to the lack of available samples ($D > 600$ Å) the experimental studies have not yet been performed.

It is also clear that the present work can be easily extended to other systems. For instance, $Si/Si_{1-x}Ge_x$ superlattices whose acoustic velocities are larger than those of GaAs-AlAs could be even better candidates for experimental investigation. Though such systems have already been studied, we think that new improvements can be carried out in light of the results of the present paper and the theory of Ref. 1 (observation of modes at frequency lower than the Brillouin lines for $Q > 1$, verification of a better agreement between theory and experiments for the relative intensity of folded and direct acoustic modes).

[1]J. He, B. Djafari-Rouhani, and J. Sapriel, preceding paper, Phys. Rev. B **37**, 4086 (1988).

[2]C. Colvard, T. A. Grant, M. V. Klein, R. Fisher, H. Morkoc, and A. C. Gossard, Phys. Rev. B **31**, 2080 (1985).

[3]J. Sapriel, J. C. Michel, J. C. Toledano, R. Vacher, J. Kervarec, and A. Regreny, Phys. Rev. B **28**, 2007 (1983).

[4]B. Jusserand, D. Paquet, F. Mollot, F. Alexandre, and G. Le Roux, Phys. Rev. B **35**, 2808 (1987).

[5]J. Sapriel, J. Chavignon, F. Alexandre, and R. Azoulay, Phys. Rev. B **34**, 7118 (1986).

[6]M. W. C. Dharma-wardana, D. J. Lockwood, J. M. Baribeau, and D. C. Houghton, Phys. Rev. B **34**, 3034 (1986); D. J. Lockwood, M. W. C. Dharma-wardana, J. M. Baribeau, and D. C. Houghton, Phys. Rev. B **35**, 2243 (1987).

[7]S. M. Rytov, Akust. Zh. **2**, 71 (1956) [Sov. Phys.—Acoust. **2**, 68 (1956)]; J. Sapriel, B. Djafari-Rouhani, and L. Dobrzynski, Surf. Sci. **126**, 197 (1983).

[8]J. F. Nye, *Physical Properties of Crystals* (Clarendon, Oxford,

1960).

[9]J. Sapriel, J. He, J. Chavignon, F. Alexandre, R. Azoulay, G. Le Roux, J. Burgeat, and R. Vacher, in *Proceedings of the European Materials Research Society, Strasbourg, June, 1986,* edited by P. A. Glasow, Y. I. Nissim, T.-P. Noblanc, and T. Speight (Les Editions de Physique, Paris, 1986); see also *Proceedings of the International Conference on the Physics of Semiconductors, Stockholm, 1986,* edited by O. Engström (World Scientific, Singapore, 1987), p. 723, and references therein.

[10]A. K. Sood, J. Menendez, M. Cardona, and K. Ploog, Phys. Rev. Lett. **54**, 2111 (1985).

[11]B. Djafari-Rouhani and J. Sapriel, Phys. Rev. B **34**, 7114 (1986).

[12]*Semiconductors: Physics of Group IV Elements and III-V Compounds,* Vol. 17a of *Landolt-Börnstein* (Springer-Verlag, Berlin, 1982).